Atmos. Chem. Phys. Discuss., 15, 8151–8189, 2015
www.atmos-chem-phys-discuss.net/15/8151/2015/
doi:10.5194/acpd-15-8151-2015
© Author(s) 2015. CC Attribution 3.0 License.

Atmospheric Chemistry and Physics Discussions

This discussion paper is/has been under review for the journal Atmospheric Chemistry and Physics (ACP). Please refer to the corresponding final paper in ACP if available.

Airborne measurements of new particle formation in the free troposphere above the Mediterranean Sea during the HYMEX campaign

C. Rose[1], K. Sellegri[1], E. Freney[1], R. Dupuy[1], A. Colomb[1], J.-M. Pichon[1], M. Ribeiro[1], T. Bourianne[2], F. Burnet[2], and A. Schwarzenboeck[1]

[1]Laboratoire de Météorologie Physique CNRS UMR6016, Observatoire de Physique du Globe de Clermont-Ferrand, Université Blaise Pascal, Clermont-Ferrand, France
[2]Centre National de Recherches Météorologiques – Groupe d'étude de l'Atmosphère Météorologique, Meteo France/CNRS, Toulouse, France

Received: 26 January 2015 – Accepted: 25 February 2015 – Published: 18 March 2015

Correspondence to: C. Rose (c.rose@opgc.univ-bpclermont.fr) and K. Sellegri (k.sellegri@opgc.univ-bpclermont.fr)

Published by Copernicus Publications on behalf of the European Geosciences Union.

Abstract

While atmospheric new particle formation (NPF) has been observed in various environments and was found to contribute significantly to the total aerosol particle concentration, the production of new particles over open seas is poorly documented in the literature. Nucleation events were detected and analysed over the Mediterranean Sea using two condensation particle counters and a Scanning Mobility Particle Sizer on-board the ATR-42 research aircraft during flights conducted between the 11 September and the 4 November 2012 in the framework of the HYMEX (HYdrological cycle in Mediterranean EXperiment) project. The main purpose of the present work was to characterize the spatial extent of the NPF process. Our findings show that nucleation is occurring over large areas above the Mediterranean Sea in all air mass types. Maximum concentrations of particles in the size range 5–10 nm (N_{5-10}) do not systematically coincide with lower fetches (time spent by the air mass over the sea before sampling), and significant N_{5-10} values are found for fetches between 0 and 60 h depending on the air mass type. These observations suggest that nucleation events could be more influenced by processes occurring above the sea, rather than linked to synoptic history. The analysis of the vertical extent of nucleation demonstrates that the process is favoured at high altitude, above 1000 m, i.e. frequently in the free troposphere, and more especially between 2000 and 3000 m, where the nucleation frequency is close to 50 %. This vertical distribution of nucleation is favoured by the gradients of several parameters, such as the condensation sink, the temperature and the relative humidity. The mixing of two air parcels could also explain the occurrence of nucleation at preferential altitudes. After they formed, particles slowly grow at high altitude to diameters of at least 30 nm while being poorly depleted by coagulation processes. Our analysis of the particle size distributions suggests that particle growth could decrease with increasing altitudes.

ACPD
15, 8151–8189, 2015

1 Introduction

New particle formation (NPF) is a widespread phenomenon in the atmosphere which results from a complex sequence of multiple processes including two major steps (Kulmala and Kerminen, 2008): (1) the formation of clusters from the gaseous phase and (2) the growth of these clusters up to sizes at which they may influence the climate through cloud related radiative processes (Kerminen et al., 2012; Makkonen et al., 2012). Observations of the phenomenon in various environments are reported in the literature (Kulmala et al., 2004), including boundary layer (BL) polluted locations (e.g. Brock et al., 2003; Wiedensohler et al., 2009), clean or rural sites (e.g. Suni et al., 2008), high altitude stations (e.g. Venzac et al., 2008; Boulon et al., 2010; Rose et al., 2014), polar areas (e.g. Asmi et al., 2010), and coastal sites (e.g. O'Dowd et al., 1998, 2002). NPF events characteristics, such as spatial extent, both vertical and horizontal (Crumeyrolle et al., 2010; Boulon et al., 2011), particle formation and growth rates (Manninen et al., 2010; Yli-Juuti et al., 2011) are known to be affected by atmospheric parameters, including the amount of gaseous precursors, the concentration of pre-existing aerosol particles and meteorological variables (temperature, relative humidity, solar radiation). However, current knowledge of the theory that lays beyond NPF remains poor, especially at high altitudes, and a more profound understanding of the mechanisms and precursors involved in nucleation and particle growth is currently required, especially to improve the accuracy of climate modelling studies.

Marine aerosol particles, as one of the main contributors to the natural aerosol emissions, has focussed the attention of the scientific community for several decades (e.g. Heintzenberg et al., 2000 and references therein). In these pristine environments, changes in the aerosol burden might have significant impacts on cloud properties, as shown by recent studies (Tao et al., 2012; Koren et al., 2014; Rosenfeld et al., 2014). Marine aerosol has a primary component, known as "sea spray aerosol", which results from the interaction between wind and water surface, and a secondary component, which is in the scope of the present work. Current knowledge regarding NPF in the

ACPD
15, 8151–8189, 2015

marine boundary layer mainly concerns coastal regions (O'Dowd et al., 1998, 2002, 2007), where observations of NPF are more abundant than over the open ocean. Many studies have concentrated on the comprehension of the mechanisms and the identification of the precursors involved in the NPF process from coastal magroalgea fields (O'Dowd and Leeuw, 2007 and references therein), including both model studies (Pirjola et al., 2000) and chamber experiments (Sellegri et al., 2005). A schematic view of the marine aerosol production in coastal areas based on observations from the Mace Head station (Ireland) is given by Vaattovaara et al. (2006). In contrast, the scarcity of open ocean nucleation studies reported in the literature might indicate that the NPF process does not occur with a high probability over open ocean.

While ground based stations allow indirect analysis of the horizontal extent of NPF (Kristensson et al., 2014; Rose et al., 2015), airborne aerosol measurements can add relevant information both on the horizontal and on the vertical extent of NPF. Such measurements were conducted over the boreal environment, in the vicinity of the Hyytiälä SMEAR-II station, using aircrafts (O'Dowd et al., 2009; Schobesberger et al., 2013) but also motorized hang glider/microlight aircraft (Junkermann, 2001, 2005) or balloons (Boy et al., 2004; Laakso et al., 2007). These studies, based on a limited number of observations, delivered contrasting results indicating that nucleation could occur throughout the boundary layer, but also in the free troposphere in some cases (Laakso et al., 2007), with no clear trend or preference. Airborne studies conducted in different environments are also reported in the literature, showing evidence for the occurrence of NPF in the free troposphere above Europe during the EUCAARI-LONGREX project (Mirme et al., 2010) and above the Arctic region, up to 7 km, by Khosrawi et al. (2010) during the project ASTAR 2004. In contrast, using a restricted number of aircraft vertical soundings, Crumeyrolle et al. (2010) suggest that over the North Sea, NPF could be limited to the top of the boundary layer.

Giving more insights in the vertical development of the NPF process in the marine troposphere is one of the main objectives of the present study based on aircraft measurements conducted above the Mediterranean sea between the 11 September and

ACPD
15, 8151–8189, 2015

the 4 November 2012 in the framework of the HYMEX (HYdrological cycle in Mediterranean EXperiment) project. We report particle size distributions and concentrations measured with a Scanning Mobility Particle Sizer (SMPS) and Condensation Particle Counters (CPC) deployed on board the French ATR-42 aircraft. The occurrence of NPF is investigated, with a special focus on the horizontal and vertical extents of the process, coupled with an analysis of several atmospheric parameters expected to explain these extents.

2 Measurements and methods

2.1 Instruments on board ATR-42 aircraft

As part of the HYMEX project, the ATR-42 research aircraft operated by SAFIRE (Service des Avions Français Instrumentés pour la Recherche en Environnement) was based at Montpellier airport, in the south of France. A total of 28 flights were performed between the 11 September and 4 November 2012 (Table 1).

The instrumental setup deployed on board and used for the analysis of NPF consisted of two Condensational Particle Counters (CPC) and a Scanning Mobility Particle Sizer (SMPS). The CPCs, developed at the Max Planck Institute for Polymer Research, Mainz, Germany, are specifically dedicated to aircraft measurements (Weigel et al., 2009). Their nominal 50 % lower cut-off diameter can be varied by changing the temperature difference between saturator and condenser. During HYMEX, one of the CPCs was measuring with a cut-off diameter of 5 nm and the second with a cut-off diameter of 10 nm. The time resolution of the CPCs was set to 1 s. The SMPS system was previously described in Crumeyrolle et al. (2010) and consists of a CPC (TSI, 3010), a Differential Mobility Analyzer (DMA) and a krypton aerosol neutralizer. The SMPS provided particle size distributions in the diameter range 20–485 nm, with a time resolution of 130 s.

ACPD
15, 8151–8189, 2015

The ATR-42 was also equipped with additional instruments dedicated to the analysis of aerosol and cloud properties: Particle Soot Absorption Photometer (PSAP, Bond et al., 1999), Optical Particle Counter (OPC, GRIMM), a compact Aerosol time of flight Mass Spectrometer (AMS, Drewnick et al., 2005) and Fast Forward Scattering Spectrometer Probe (Fast-FSSP). The aerosol instrumentation was connected to the community aerosol inlet (CAI) which has a 50 % sampling efficiency for particles larger than 5 µm (see Crumeyrolle et al., 2010 and references therein for more details). Routine meteorological variables were continuously monitored.

2.2 Data analysis

2.2.1 Sea/land mask

The main objective of this study was to investigate the occurrence of NPF in the marine troposphere. For that purpose, all measurements conducted above land were removed from the database. An arbitrary threshold distance of 1 km to the coast was set to consider measurement as "marine". The distance D between two geographical points A and B, knowing their coordinates, was calculated according to:

$$D = \arccos(\sin(\phi_A) \times \sin(\phi_B) + \cos(\phi_A) \times \cos(\phi_B) \times \cos(\lambda_A - \lambda_B)) \times R_T \quad (1)$$

Where ϕ_Y and λ_Y are the latitude and longitude of the location Y, respectively, and $R_T = 6371$ km is the mean radius of the Earth. The position of the points located at the threshold distance of 1000 ± 50 m from the aircraft position was calculated using Eq. (1) every 10 s along the flight path (which correspond to a distance of 1 km for a typical aircraft speed of 100 m s^{-1}) and plotted on a map. Measurements were considered as "marine" when none of these points (forming an ellipse) intercepted any coastline, as illustrated on Fig. 1. We finally assumed that the flag ("marine" or "land") obtained at a time t was the same for the 5 s that preceded t and the 4 s that followed t.

ACPD
15, 8151–8189, 2015

2.2.2 Detection of nucleation events

In order to track the occurrence of nucleation above the Mediterranean Sea and to evaluate the strength of the events, particle concentration in the size range 5–10 nm (N_{5-10}) was calculated by subtracting the data readings of the two CPCs. After analysing the variability of N_{5-10} apart from nucleation periods, we found that N_{5-10} concentrations had an average value of 29.9 cm^{-3} and a SD of 144.8 cm^{-3}. Hence, N_{5-10} concentrations were considered significant above the threshold value of 175 cm^{-3}. It is worth noticing that in-cloud measurements were filtered out in order to prevent the detection of elevated particle concentrations that could be sampling artefacts linked to the fragmentation of cloud droplets impacting the aerosol inlet (Weber et al., 1998).

2.2.3 Air mass back trajectories

The influence of air mass history on the occurrence of nucleation was studied using three days air mass back trajectories computed with the HYSPLIT transport and dispersion model (Draxler and Rolph, 2003). Three days before sampling were chosen based on previous work by Tunved et al. (2005) who estimated the turnover time of aerosol particles to be around 1.6–1.7 days for nuclei size ranges and 2.4 days for 200 nm particles. Back trajectories were calculated every 5 min along the flight path (i.e. 30 km for a typical aircraft speed of 100 $m\,s^{-1}$) and air masses were further classified into Northern Europe, Western Europe, Southern Mediterranean Sea, Eastern Mediterranean Sea and Local types according to the maximum time spent in each sector. As illustrated on Fig. 2, the Local sector corresponds to the geographical area were most of the flights took place during the HYMEX campaign (centred on the position 41.6701°/6.8769°), while Northern Europe, Western Europe, Southern Mediterranean Sea and Eastern Mediterranean Sea types are related to the sectors 45–135°, 135–225°, 225–315° and 315–45°, respectively. We made the assumption that the air mass origin obtained at a time t was the same for the 150 s that preceded t and the 149 s that followed t.

ACPD
15, 8151–8189, 2015

3 Results and discussion

3.1 Observation of nucleation events above the Mediterranean Sea

3.1.1 Horizontal extent

When considering all measurements recorded in clear sky conditions above the sea, 25 % of N_{5-10} concentrations were found to exceed the threshold value. These concentrations are obtained at all times, with slightly increased probabilities during the periods 11:00–17:00 and 17:00–05:00 UTC (~ 27 %) compared to early hours (05:00–11:00 UTC, 23 %). The fact that night time could be associated to higher probabilities for the detection of significant N_{5-10} values compared to morning hours was quite unexpected since nucleation events are more frequently reported to be initiated in the morning (e.g. Dal Maso et al., 2005; Rose et al., 2015). In fact, night time events have already been observed, but appear to be more scarce (Lee et al., 2008; Suni et al., 2008). The origin of nanoparticles observed at night in the present study is further discussed in Sect. 3.2.2.

The location where the significant N_{5-10} concentrations (> 175 cm^{-3}) were detected is shown on Fig. 3. The map we obtain clearly indicates that nanoparticle concentrations are detected above the sea over large areas, being continuously detected along the flight paths over distances that can reach ~ 580 km (flight 52). N_{5-10} concentrations are in the range 236 (25th perc.)–564 (75th perc.) cm^{-3}, with a median value of 329 cm^{-3}. This range is of the order of magnitude of concentrations measured by the SMPS for larger particles (Table A1) at high altitudes, which indicates that nucleation may contribute significantly to the total aerosol burden after they have grown.

According to the geographical distribution of the nucleation points in Fig. 3, it is likely that nucleation could occur at variable distances to the coast. Small particles observed close to the littoral may be expected to be produced during events initiated above land or involving gaseous precursors originating from the continental boundary layer (BL). In contrast, significant N_{5-10} concentrations measured hundreds of kilometres far from the

ACPD
15, 8151–8189, 2015

shore suggest the occurrence of events which are more disconnected from continental sources, and could be rather associated with marine precursors. This point is further discussed in the following section.

3.1.2 Influence of air mass origin – fetch of air masses

As reported in Table 1, most of the studied flights were performed under Western Europe and Southern Mediterranean Sea atmospheric flows (15 and 7 out of 28, respectively), while northern and local types were only observed during three flights. The three remaining flights were performed under variable conditions, however often dominated by Western Europe and Southern Mediterranean Sea flows.

Significant concentrations of small particles in the size range 5–10 nm were detected in all types of air masses (Table 2), but the highest nucleation probability was found in northern air masses, where 60 % of N_{5-10} values exceeded the threshold value. In contrast, Eastern Mediterranean Sea flows showed the lowest nucleation probability, of around 0.3 %. However, the values obtained for eastern, northern and local air masses may not be relevant as we have very little statistics on them. For this reason, eastern, northern and local flows will not be further discussed. In Western Europe and South Mediterranean Sea air masses, the N_{5-10} threshold value was exceeded in 11 and 32 % of the cases studied, respectively. It is worth noticing that the frequency of occurrence of significant ultrafine particle concentrations is relatively important in southern air masses, i.e. in air masses that have spent a significant time over the Mediterranean Sea, free of the influence of recent continental emissions.

Median N_{5-10} concentrations calculated for western and southern flows were on average very similar, 300 and 362 cm^{-3}, respectively. Based on the interquartile range (IQR), the variability of N_{5-10} concentrations was relatively low for these two air mass types (IQR = 332 and 324 cm^{-3}, respectively). These results suggest that the strength of the events and the number of nucleated particles are not deeply impacted by air mass origin, and could instead be influenced by local (marine) atmospheric conditions.

ACPD
15, 8151–8189, 2015

In order to further investigate this aspect, a more detailed analysis of the number of nucleated particles as a function of the fetch, i.e. the time spent by air masses above the sea before sampling, was conducted and is reported on Fig. 4, separately for Western Europe and South Mediterranean Sea flows. Reported $N_{5–10}$ are averaged concentrations calculated from the 60 s periods spanning around the times used for air mass back trajectories computation.

In Western Europe and South Mediterranean Sea air masses, fetches up to 60 h were calculated. In these air masses, larger concentrations are typically recorded for smaller fetches, with maximum $N_{5–10}$ values obtained for fetches around 5 h. This last observation could either indicate that events are influenced by precursors from marine origin and have a growth rate higher than 0.8 nm h^{-1}, or that the detected clusters were produced over the continent and need 4 to 5 h before being detected by our CPC tandem. However, we do detect significant concentrations of particles in the 5–10 nm size range in air masses with fetches up to 60 h, which clearly suggests a significant marine contribution for these events and would indicate that the Mediterranean troposphere houses precursors of nucleation.

The purpose of the next section is now to investigate the vertical extent of nucleation.

3.1.3 Vertical extent

A total of 40 vertical soundings were performed during the studied flights, giving the opportunity to examine profiles of the $N_{5–10}$ particle concentrations. Such profiles are shown in Fig. 5. Boundary layer height (BLH) is also provided as additional information for each sounding. BLH was obtained using interpolation in space and time from the diagnosed BLH retrieved by the European Centre for Medium Range Weather Forecasts (ECMWF) at forecast times of 3, 6, 9, 12, 15, 18, 21 and 24 h, starting at 00:00 UTC, and horizontal resolution 0.25°. Estimations of the BLH were also obtained from the analysis of the vertical gradients of temperature, potential temperature, relative humidity and specific humidity, as suggested by Seidel et al. (2010). Reasonable agreement was found between the "gradient method" and ECMWF BLHs.

ACPD
15, 8151–8189, 2015

For most of the soundings, the BLH was lower than 1000 m, being on average 657 ± 323 m. Fifteen profiles shown on Fig. 5 are not sufficient to allow a complete vertical investigation of both boundary layer (BL) and free troposphere (FT) altitudes and were thus left out (profiles no. 1, 7, 8, 11, 15, 16, 17, 21, 22, 23, 24, 25, 26, 38 and 40). For 17 of the 25 remaining profiles, N_{5-10} concentrations exceeding the threshold value are mainly found above the BL, indicating the occurrence of nucleation in the FT (profiles no. 2, 6, 14, 18, 19, 20, 27, 28, 30, 31, 32, 33, 34, 35, 36, 37 and 39). Only 3 profiles (no. 3, 4, 5), obtained during take-off/landing phases, show the opposite, with nucleation events triggered within the BL. Nucleation is observed both in the BL and in the FT with no preferential altitudes identified during two soundings (no. 12 and 29), and three profiles do not show any indication of nucleation (no. 9, 10 and 13).

The vertical limits of the nucleation process are clearly visible for profiles no. 6 and 28. For profile no. 6, nucleation is observed between 1680 and 3170 m, with concentrations significantly increased between 2400 and 2900 m. During sounding no. 28, nucleation is detected on a slightly more restricted altitude range, 1350–1780 m, with higher concentrations between 1660 and 1710 m. Other profiles, such as no. 19, 24 and 35, also display N_{5-10} values which are significantly increased on a well defined atmospheric layer above 1000 m, not only indicating that nucleation could be promoted at high altitudes, but also suggesting the existence of preferential altitudes.

In order to further investigate the vertical extension of nucleation, all measurements were considered, i.e. N_{5-10} concentrations measured during vertical soundings and also at constant altitude levels. Figure 6 (left panel) shows the percentage of N_{5-10} concentrations exceeding the threshold value as a function of altitude range. As previously suggested by Fig. 5, nucleation seems to be favoured above 1000 m. In fact, below 1000 m, less than 4 % of the recorded concentrations were found to be significant. In contrast, nucleation probability is increased by 10 above 1000 m, and it is worth noticing that almost 50 % of the concentrations obtained between 2000 and 3000 m exceed the threshold value, indicating that these altitudes could more especially favour the occurrence of nucleation.

ACPD
15, 8151–8189, 2015

However, it seems that when nucleation events are detected, the number of nucleated particles does not significantly vary with altitude, especially above 500 m, where median concentrations are in the range 309–376 cm^{-3} (Fig. 6, right panel). Below 500 m, N_{5-10} are slightly increased and show higher variability, which might be caused by more inhomogeneous conditions found in this part of the atmosphere compared to higher altitudes.

The fact that nucleation is favoured in the FT compared to the BL contradicts the results by Crumeyrolle et al. (2010), who found that NPF events were limited to the top of the BL in the North Sea. However it is worth noticing that the number of vertical profiles included in the Crumeyrolles study was limited (13 profiles), and most of them were performed close to the coast.

3.1.4 Why such a vertical extension?

The purpose of this section is to investigate atmospheric parameters which are expected to support the highest probability for nucleation to occur at high altitude.

Figure 7 shows, for the different altitude ranges previously introduced, the median condensation sink (CS) calculated from SMPS size distributions recorded at constant altitudes, i.e. apart from vertical soundings. Up to 2000 m, the median CS does not significantly vary with altitude, being in the range 3.1–3.9 $\times 10^{-3}$ s^{-1}. A higher variability observed below 500 m could again be explained by more inhomogeneous conditions found at low altitudes. Above 2000 m, CS values are significantly decreased, with median values below 10^{-3} s^{-1}. These first observations suggest that higher nucleation frequencies found above 2000 m could be, at least partly, explained by lower CS. The fact that nucleation could be promoted at high altitude due to lower CS values was also reported by Boulon et al. (2011) at the puy de Dôme (PUY) station (1465 m a.s.l., France), where NPF is observed twice as frequently as at the BL station of Opme (660 m a.s.l.) located 12 km south east of the PUY.

A more complete analysis focussed on altitudes above 2000 m was then conducted to highlight the role of the CS in the nucleation process at high altitude. Figure 8 shows

ACPD
15, 8151–8189, 2015

the correlation between $N_{5–10}$ particle concentration and CS, separately for the two altitude ranges above 2000 m. The $N_{5–10}$ shown are 130 s averaged values coinciding with SMPS measurements used for the CS calculation. Based on Fig. 8, we observe that ultrafine particle concentration and CS are positively correlated, especially between 2000 and 3000 m (R^2 = 0.48). The lack of measurements did not allow similar analysis at lower altitudes to compare with, but the fact that at high altitude, where the CS is usually low compared to BL stations, increased CS could favour the occurrence of nucleation has already been reported in the literature (Boulon et al., 2010; Rose et al., 2014). While lower CS values are typically reported on event days compared to non-event days at BL sites, increased CS are found on event days at high altitude stations (Manninen et al., 2010). We may hypothesis that some gaseous compounds are transported, together with the pre-existing particles, from lower altitudes, and that they may be further oxidized to more condensable species involved in the nucleation process.

Other parameters, such as temperature and relative humidity (RH) were previously reported to influence the nucleation process. While low temperatures were found to favor nucleation (Young et al., 2007), the role of RH seems to be more ambiguous. In fact, nucleation is likely to occur preferentially at low RH (Birmili et al., 2003), and both the nucleation rate and nucleated cluster concentration are reported to be anti-correlated with RH (Jeong et al., 2004; Sihto et al., 2006). However, nucleation events have been detected in the vicinity of clouds, where high RH are found (Clarke et al., 1998). Another aspect to consider is that among high altitudes air masses, increased RH would also be associated to intrusions from the BL and hence more gaseous precursors and higher CS.

Statistics concerning temperature and RH recorded during the studied flights are presented as a function of altitude range on Fig. 9. It is very clear that temperature is decreasing with altitude, especially above 3000 m where most of the temperatures are found to be negative. The same trend is observed for RH, but with higher variability. $N_{5–10}$ concentrations were also directly considered as a function of temperature, RH

ACPD
15, 8151–8189, 2015

and humidity mixing ratio ($g\,kg^{-1}$), but the correlations between these meteorological parameters and the particle concentration was weak at all altitudes ($|R^2| < 0.2$).

Beside their individual influence on the nucleation process, the different parameters considered in the previous analysis might also have a collective indirect effect. Indeed, it has been previously reported by several studies that the mixing of two air parcels showing contrasting levels of RH, temperature, condensation sink and precursors, could favor the occurrence of nucleation (Nilsson and Kulmala, 1998; Khosrawi and Konopka, 2003; Dall'Osto et al., 2013).

Global radiation, which is expected to be more intense at high altitude, and thus favor photochemical processes, including oxidation of gaseous precursors involved in the nucleation process, could also give additional explanation to the observed vertical distribution of the nucleation process.

We have shown so far that above the Mediterranean Sea, nucleation was observed over large areas and could be favoured at high altitude, since particles in the size range 5–10 nm are mostly seen above 1000 m. The purpose of the next section is to investigate the growth of these particles to larger diameters at high altitudes by analysing the shape of the SMPS size distributions.

3.2 Investigation of particle growth at high altitude

3.2.1 Analysis of SMPS particle size distributions

All SMPS size distributions (20.4–484.5 nm) recorded at constant altitude were fitted with four Gaussian modes: a nucleation mode with a mean diameter around 25 nm, an Aitken mode with a mean diameter around 50 nm, a first accumulation mode with a mean diameter around 110 nm and a second accumulation mode centred around 220 nm as initial guesses. These four modes were chosen because they most frequently came out of the fitting procedure when run without initial guesses. These diameters were previously found in the literature to describe particle size distributions in the marine atmosphere (Heintzenberg et al., 2000). The geometric mean diameters

ACPD
15, 8151–8189, 2015

of these modes found by the fitting procedure vary from the initial guesses with time and altitude. In the following sections, the parameters of the modes (geometric mean diameter and concentration) will be used to describe the evolution of the particle size distribution.

Figure 10 shows the average fitted distributions as a function of altitude and daytime. The analysis is focussed on the highest altitude ranges, where nucleation was more frequently observed (the altitude range 1000–2000 m is not considered because of a too small number of data points). The parameters of the Gaussians used for these fits are given as additional information in Table A1. During the time period 11:00–17:00 UTC, the size distributions are dominated by the nucleation mode, which contribution to the total particle concentration is 42 % between 2000 and 3000 m and 48 % above 3000 m. However, both the concentration and the diameter of the nucleation mode appear to be larger between 2000 and 3000 m compared to higher altitudes (Table A1). Since $N_{5–10}$ concentrations were shown to be comparable for the two altitude ranges (Fig. 7), a faster growth at lower altitudes supported by a larger pool of condensable species could explain the differences observed on the size distributions.

At night (17:00–05:00 UTC), the contributions of nucleation and Aitken modes to the total particle concentration are very similar between 2000 and 3000 m, being around 34 %, whereas above 3000 m the nucleation mode remains dominant (46 % against 36 % for the Aitken mode). Again, this observation suggests that particle growth could get slower with increasing altitudes.

In the morning (05:00–11:00 UTC), the average size distribution above 3000 m displays a nucleation mode which diameter is similar to the diameter observed at night (~ 23 nm), and with a contribution to the total particle concentration which is significantly higher than the contribution of the Aitken mode (60 and 23 %, respectively). In contrast, between 2000 and 3000 m, the nucleation mode displays a large diameter (30.5 nm) and a contribution which is lower than the contribution of the Aitken mode (30 and 51 %, respectively). We may hypothesis that the small particles which are seen in the nucleation mode above 3000 m do not originate from nucleation events initiated in

ACPD
15, 8151–8189, 2015

the morning, but were rather formed the day before and are still undergoing a very slow growth process. The low concentration of nucleation mode particles between 2000 and 3000 m might be explained by a faster growth for the particles formed the day before, which have thus reached larger diameters, and also by the fact that particles nucleated in the morning (the nucleation probability between 2000 and 3000 m during the time period 05:00–11:00 UTC is 22 %) may not have already reached the lower detection limit of the SMPS.

3.2.2 Origin of night time nanoparticles

As previously mentioned, nanoparticles in the size range 5–10 nm were detected during night time (17:00–05:00 UTC). The purpose of this last section is to investigate their origin, and more particularly to examine the possibility for the night time particles to originate from nucleation events triggered earlier during day time.

The time interval 09:00–12:00 UTC, during which the formation of cluster particles is most frequently observed (Rose et al., 2014, 2015), was considered as a reference nucleation period, and only the significant 130 s averaged N_{5-10} concentrations obtained between 09:00 and 12:00 UTC were further considered. We estimated the half-life time of these particles, i.e. the time t_{fin} at which these concentrations reached half of their initial values, obtained at t_0, under the following assumptions: (1) particles are removed from the size range 5–10 nm by coagulation and growth processes and (2) the coagulation sink calculated at t_0 is constant during particle growth. t_{fin} is finally given by Eq. (2):

$$t_{fin} = t_0 + \frac{0.5}{\mathrm{Coag} + \frac{f}{5} \cdot \mathrm{GR}} \quad (2)$$

Where Coag is the coagulation sink of 5 nm particles derived from SMPS data, and GR is the particle growth rate. The factor f represents the fraction of the aerosol population which is activated for growth, and was assumed to be equal to unity.

ACPD
15, 8151–8189, 2015

Particle GR were estimated from the average shift of the nucleation mode diameter observed on the SMPS size distributions between night time (17:00–05:00 UTC) and morning hours (05:00–11:00 UTC) for the altitude range 2000–3000 m (Table A1, Fig. 10). An average value of 0.31 nm h^{-1} was found. However, GR was previously reported to increase with particle size (Yli-Juuti et al., 2011; Kulmala et al., 2013), this is the reason why lower GR of 0.1 nm h^{-1} was also used to describe particle growth in the size range 5–10 nm. In order to complete our sensitivity study regarding the GR, additional higher value of 1 nm h^{-1} was selected. The results of this analysis are reported on Fig. 11, which first indicates that particle life time increases with altitude, which might be explained by decreasing coagulation sinks. Considering the scenario with intermediate GR of 0.3 nm h^{-1}, initial N_{5-10} concentrations are all divided by two before night time, suggesting that, considering the relatively high concentrations found at night, there would be an additional source of 5–10 nm particles at high altitudes. The same conclusion is obtained with GR = 1 nm h^{-1}. In contrast, using the more probable value of GR = 0.1 nm h^{-1}, we observe that for some cases, nanoparticle concentration reach half of their initial value only after 17:00 UTC, or even later. Because of the reduced number of data points, these conclusions must be considered with caution but it is likely that a large fraction of nanoparticles detected during the night were formed earlier during the day. The subsistence of the nanoparticles in the size range 5–10 nm might be explained by low coagulation sinks coupled with slow particle growth.

4 Conclusions

We investigated the occurrence of nucleation events above the Mediterranean Sea using data obtained during research flights performed in the framework of the HYMEX project between September and November 2012.

Based on our observations, nucleation takes place over large areas above the Mediterranean Sea in all air mass types. Nucleation probability slightly varies with air mass origin, but the signature of the different air mass types is however complex to dis-

ACPD
15, 8151–8189, 2015

tinguish in terms of N_{5-10} concentrations. In Western Europe and South Mediterranean Sea flows, more frequently observed compared to other air mass types, maximum concentrations were obtained for fetches around 5 h, but significant concentrations persist over fetches up to 60 h, suggesting that the nucleation process could be more influenced by parameters inherent of the marine troposphere.

The analysis of the vertical extension of nucleation showed that the process was promoted at high altitude, above 1000 m, and especially between 2000 and 3000 m. Simultaneous analysis of the boundary layer height indicated that these altitudes often corresponded to free tropospheric conditions. Vertical gradient of the condensation sink, together with temperature and humidity might explain the increasing nucleation probability with altitude. The mixing of two air parcels with contrasting properties (temperature, RH, condensation sink, precursors) could also explain the occurrence of nucleation at preferential altitudes. However, for a given high altitude range, larger N_{5-10} concentrations were found for larger CS, likely associated with higher oxidation of gas phase precursors.

The investigation of the global shape of the particle size distributions derived from SMPS measurements finally allowed us to study the particle growth above 2000 m, and more particularly the relative contribution of the different particle modes to the total concentration as a function of time and altitude. After they formed, particles appear to grow to larger sizes above 2000 m, reaching the Aitken mode range, but with growth rates which seem to decrease with altitude. This slow growth, coupled with low coagulation sinks, may favour longer subsistence for nanoparticles in the size range 5–10 nm, and could explain the detection of these small particles during night time, several hours after their formation.

Our findings demonstrate that high altitude could promote the occurrence of NPF, not only over continental areas, as previously suggested by Boulon et al. (2011), but also over open seas, with indications of marine precursors. This result supports the model study by Makkonen et al. (2012), which predicts that nucleation could have a significant contribution to the cloud condensation nuclei (CCN) concentration over the Mediter-

ACPD
15, 8151–8189, 2015

ranean Sea, and indicates that this contribution could be even more decisive at high altitude, where clouds form.

Acknowledgements. HyMeX SOP1 was supported by CNRS, Météo-France, CNES, IRSTEA, INRA through the large interdisciplinary international program MISTRALS (Mediterranean Integrated STudies at Regional And Local Scales) dedicated to the understanding of the Mediterranean Basin environmental process (http://www.mistrals-home.org). We also would like to thank SAFIRE for their support during instrument integration on the French ATR-42 and HYMEX SOP1 campaign execution. We finally gratefully acknowledge the NOAA Air Resource Laboratory (ARL) for the provision of the HYSPLIT READY website (http://www.arl.noaa.gov/ready.php) used in this publication for calculating the trajectories.

References

Asmi, E., Frey, A., Virkkula, A., Ehn, M., Manninen, H. E., Timonen, H., Tolonen-Kivimäki, O., Aurela, M., Hillamo, R., and Kulmala, M.: Hygroscopicity and chemical composition of Antarctic sub-micrometre aerosol particles and observations of new particle formation, Atmos. Chem. Phys., 10, 4253–4271, doi:10.5194/acp-10-4253-2010, 2010.

Birmili, W., Berresheim, H., Plass-Dülmer, C., Elste, T., Gilge, S., Wiedensohler, A., and Uhrner, U.: The Hohenpeissenberg aerosol formation experiment (HAFEX): a long-term study including size-resolved aerosol, H_2SO_4, OH, and monoterpenes measurements, Atmos. Chem. Phys., 3, 361–376, doi:10.5194/acp-3-361-2003, 2003.

Bond, T. C., Anderson, T. L., and Campbell, D.: Calibration and intercomparison of filter-based measurements of visible light absorption by aerosols, Aerosol Sci. Tech., 30, 582–600, 1999.

Boulon, J., Sellegri, K., Hervo, M., Picard, D., Pichon, J.-M., Fréville, P., and Laj, P.: Investigation of nucleation events vertical extent: a long term study at two different altitude sites, Atmos. Chem. Phys., 11, 5625–5639, doi:10.5194/acp-11-5625-2011, 2011.

Boulon, J., Sellegri, K., Venzac, H., Picard, D., Weingartner, E., Wehrle, G., Collaud Coen, M., Bütikofer, R., Flückiger, E., Baltensperger, U., and Laj, P.: New particle formation and ultrafine charged aerosol climatology at a high altitude site in the Alps (Jungfraujoch, 3580 m a.s.l., Switzerland), Atmos. Chem. Phys., 10, 9333–9349, doi:10.5194/acp-10-9333-2010, 2010.

Boy, M., Petäjä, T., Dal Maso, M., Rannik, Ü., Rinne, J., Aalto, P., Laaksonen, A., Vaattovaara, P., Joutsensaari, J., Hoffmann, T., Warnke, J., Apostolaki, M., Stephanou, E. G., Tsapakis, M.,

ACPD
15, 8151–8189, 2015

Kouvarakis, A., Pio, C., Carvalho, A., Römpp, A., Moortgat, G., Spirig, C., Guenther, A., Greenberg, J., Ciccioli, P., and Kulmala, M.: Overview of the field measurement campaign in Hyytiälä, August 2001 in the framework of the EU project OSOA, Atmos. Chem. Phys., 4, 657–678, doi:10.5194/acp-4-657-2004, 2004.

Brock, C. A., Trainer, M., Ryerson, T. B., Neuman, J. A., Parrish, D. D., Holloway, J. S., Nicks, D. K., Frost, G. J., Hübler, G., Fehsenfeld, F. C., Wilson, J. C., Reeves, J. M., Lafleur, B. G., Hilbert, H., Atlas, E. L., Donnelly, S. G., Schauffler, S. M., Stroud, V. R., and Wiedinmyer, C.: Particle growth in urban and industrial plumes in Texas, J. Geophys. Res., 108, 4111, doi:10.1029/2002JD002746, 2003.

Clarke, A. D., Varner, J. L., Eisele, F., Mauldin, R. L., Tanner, D., and Litchy, M.: Particle production in the remote marine atmosphere: cloud outflow and subsidence during ACE 1, J. Geophys. Res.-Atmos., 103, 16397–16409, doi:10.1029/97JD02987, 1998.

Crumeyrolle, S., Manninen, H. E., Sellegri, K., Roberts, G., Gomes, L., Kulmala, M., Weigel, R., Laj, P., and Schwarzenboeck, A.: New particle formation events measured on board the ATR-42 aircraft during the EUCAARI campaign, Atmos. Chem. Phys., 10, 6721–6735, doi:10.5194/acp-10-6721-2010, 2010.

Dall'Osto, M., Querol, X., Alastuey, A., O'Dowd, C., Harrison, R. M., Wenger, J., and Gómez-Moreno, F. J.: On the spatial distribution and evolution of ultrafine particles in Barcelona, Atmos. Chem. Phys., 13, 741–759, doi:10.5194/acp-13-741-2013, 2013.

Draxler, R. R. and Rolph, G. D.: HYSPLIT (Hybrid Single-Particle Langrangian Integrated Trajectory) model access via NOAA ARL READY website, available at: http://www.arl.noaa.gov/ready/hysplit4.html (15 January 2015), 2003.

Drewnick, F., Hings, S. S., DeCarlo, P., Jayne, J. T., Gonin, M., Fuhrer, K., Weimer, S., Jimenez, J. L., Demerjian, K. L., Borrmann, S., and Worsnop, D. R.: A new Time-of-Flight Aerosol Mass Spectrometer (TOF-AMS) – instrument description and first field deployment, Aerosol Sci. Tech., 39, 637–658, doi:10.1080/02786820500182040, 2005.

Heintzenberg, J., Covert, D. C., and Van Dingenen, R.: Size distribution and chemical composition of marine aerosols: a compilation and review, Tellus B, 52, 1104–1122, 2000.

Jeong, C.-H., Hopke, P. K., Chalupa, D., and Utell, M.: Characteristics of nucleation and growth events of ultrafine particles measured in Rochester, NY, Environ. Sci. Technol., 38, 1933–1940, doi:10.1021/es034811p, 2004.

Junkermann, W.: An ultralight aircraft as platform for research in the lower troposphere: system performance and first results from radiation transfer studies in stratiform aerosol lay-

ACPD
15, 8151–8189, 2015

ers and broken cloud conditions, J. Atmos. Ocean. Tech., 18, 934–946, doi:10.1175/1520-0426(2001)018<0934:AUAAPF>2.0.CO;2, 2001.
Junkermann, W.: The actinic UV-radiation budget during the ESCOMPTE campaign 2001: results of airborne measurements with the microlight research aircraft D-MIFU, Atmos. Res., 74, 461–475, doi:10.1016/j.atmosres.2004.06.009, 2005.
Kerminen, V.-M., Paramonov, M., Anttila, T., Riipinen, I., Fountoukis, C., Korhonen, H., Asmi, E., Laakso, L., Lihavainen, H., Swietlicki, E., Svenningsson, B., Asmi, A., Pandis, S. N., Kulmala, M., and Petäjä, T.: Cloud condensation nuclei production associated with atmospheric nucleation: a synthesis based on existing literature and new results, Atmos. Chem. Phys., 12, 12037–12059, doi:10.5194/acp-12-12037-2012, 2012.
Khosrawi, F. and Konopka, P.: Enhanced particle formation and growth due to mixing processes in the tropopause region, Atmos. Environ., 37, 903–910, 2003.
Khosrawi, F., Ström, J., Minikin, A., and Krejci, R.: Particle formation in the Arctic free troposphere during the ASTAR 2004 campaign: a case study on the influence of vertical motion on the binary homogeneous nucleation of H_2SO_4/H_2O, Atmos. Chem. Phys., 10, 1105–1120, doi:10.5194/acp-10-1105-2010, 2010.
Koren, I., Dagan, G., and Altaratz, O.: From aerosol-limited to invigoration of warm convective clouds, Science, 344, 1143–1146, doi:10.1126/science.1252595, 2014.
Kristensson, A., Johansson, M., Swietlicki, E., Kivekäs, N., Hussein, T., Nieminen, T., Kulmala, M., and Dal Maso, M.: NanoMap: geographical mapping of atmospheric new particle formation through analysis of particle number size distribution and trajectory data, Boreal Environ. Res., 19, 329–342, 2014.
Kulmala, M. and Kerminen, V.-M.: On the formation and growth of atmospheric nanoparticles, Atmos. Res., 90, 132–150, doi:10.1016/j.atmosres.2008.01.005, 2008.
Kulmala, M., Kontkanen, J., Junninen, H., Lehtipalo, K., Manninen, H. E., Nieminen, T., Petäjä, T., Sipilä, M., Schobesberger, S., Rantala, P., Franchin, A., Jokinen, T., Järvinen, E., Äijälä, M., Kangasluoma, J., Hakala, J., Aalto, P. P., Paasonen, P., Mikkilä, J., Vanhanen, J., Aalto, J., Hakola, H., Makkonen, U., Ruuskanen, T., Mauldin, R. L., Duplissy, J., Vehkamäki, H., Bäck, J., Kortelainen, A., Riipinen, I., Kurtén, T., Johnston, M. V., Smith, J. N., Ehn, M., Mentel, T. F., Lehtinen, K. E. J., Laaksonen, A., Kerminen, V.-M., and Worsnop, D. R.: Direct observations of atmospheric aerosol nucleation, Science, 339, 943–946, doi:10.1126/science.1227385, 2013.

ACPD
15, 8151–8189, 2015

Kulmala, M., Vehkamäki, H., Petäjä, T., Dal Maso, M., Lauri, A., Kerminen, V.-M., Birmili, W., and McMurry, P. H.: Formation and growth rates of ultrafine atmospheric particles: a review of observations, J. Aerosol Sci., 35, 143–176, 2004.

Laakso, L., Grönholm, T., Kulmala, L., Haapanala, S., Hirsikko, A., Lovejoy, E. R., Kazil, J., Kurten, T., Boy, M., Nilsson, E. D., Sogachev, A., Riipinen, I., Stratmann, F., and Kulmala, M.: Hot-air balloon as a platform for boundary layer profile measurements during particle formation, Boreal Environ. Res., 12, 279–294, 2007.

Lee, S.-H., Young, L.-H., Benson, D. R., Suni, T., Kulmala, M., Junninen, H., Campos, T. L., Rogers, D. C., and Jensen, J.: Observations of nighttime new particle formation in the troposphere, J. Geophys. Res.-Atmos., 113, D10210, doi:10.1029/2007JD009351, 2008.

Makkonen, R., Asmi, A., Kerminen, V.-M., Boy, M., Arneth, A., Hari, P., and Kulmala, M.: Air pollution control and decreasing new particle formation lead to strong climate warming, Atmos. Chem. Phys., 12, 1515–1524, doi:10.5194/acp-12-1515-2012, 2012.

Manninen, H. E., Nieminen, T., Asmi, E., Gagné, S., Häkkinen, S., Lehtipalo, K., Aalto, P., Vana, M., Mirme, A., Mirme, S., Hõrrak, U., Plass-Dülmer, C., Stange, G., Kiss, G., Hoffer, A., Törő, N., Moerman, M., Henzing, B., de Leeuw, G., Brinkenberg, M., Kouvarakis, G. N., Bougiatioti, A., Mihalopoulos, N., O'Dowd, C., Ceburnis, D., Arneth, A., Svenningsson, B., Swietlicki, E., Tarozzi, L., Decesari, S., Facchini, M. C., Birmili, W., Sonntag, A., Wiedensohler, A., Boulon, J., Sellegri, K., Laj, P., Gysel, M., Bukowiecki, N., Weingartner, E., Wehrle, G., Laaksonen, A., Hamed, A., Joutsensaari, J., Petäjä, T., Kerminen, V.-M., and Kulmala, M.: EUCAARI ion spectrometer measurements at 12 European sites – analysis of new particle formation events, Atmos. Chem. Phys., 10, 7907–7927, doi:10.5194/acp-10-7907-2010, 2010.

Dal Maso, M., Kulmala, M., Riipinen, I., Wagner, R., Hussein, T., Aalto, P. P., and Lehtinen, K. E.: Formation and growth of fresh atmospheric aerosols: eight years of aerosol size distribution data from SMEAR II, Hyytiala, Finland, Boreal Environ. Res., 10, 323, 2005.

Mirme, S., Mirme, A., Minikin, A., Petzold, A., Hõrrak, U., Kerminen, V.-M., and Kulmala, M.: Atmospheric sub-3 nm particles at high altitudes, Atmos. Chem. Phys., 10, 437–451, doi:10.5194/acp-10-437-2010, 2010.

Nilsson, E. D. and Kulmala, M.: The potential for atmospheric mixing processes to enhance the binary nucleation rate, J. Geophys. Res.-Atmos., 103, 1381–1389, 1998.

O'Dowd, C. D. and Leeuw, G. de: Marine aerosol production: a review of the current knowledge, Philos. T. Roy. Soc. A, 365, 1753–1774, doi:10.1098/rsta.2007.2043, 2007.

ACPD
15, 8151–8189, 2015

O'Dowd, C. D., Geever, M., Hill, M. K., Smith, M. H., and Jennings, S. G.: New particle formation: nucleation rates and spatial scales in the clean marine coastal environment, Geophys. Res. Lett., 25, 1661–1664, 1998.

O'Dowd, C. D., Hämeri, K., Mäkelä, J., Väkeva, M., Aalto, P., de Leeuw, G., Kunz, G. J., Becker, E., Hansson, H.-C., Allen, A. G., Harrison, R. M., Berresheim, H., Kleefeld, C., Geever, M., Jennings, S. G., and Kulmala, M.: Coastal new particle formation: Environmental conditions and aerosol physicochemical characteristics during nucleation bursts, J. Geophys. Res.-Atmos., 107, PAR 12-1–PAR 12-17, doi:10.1029/2000JD000206, 2002.

O'Dowd, C. D., Yoon, Y. J., Junkermann, W., Aalto, P., Kulmala, M., Lihavainen, H., and Viisanen, Y.: Airborne measurements of nucleation mode particles II: boreal forest nucleation events, Atmos. Chem. Phys., 9, 937–944, doi:10.5194/acp-9-937-2009, 2009.

Pirjola, L., O'Dowd, C. D., Brooks, I. M., and Kulmala, M.: Can new particle formation occur in the clean marine boundary layer?, J. Geophys. Res., 105, 26531–26546, doi:10.1029/2000JD900310, 2000.

Rose, C., Sellegri, K., Asmi, E., Hervo, M., Freney, E., Junninen, H., Duplissy, J., Sipilä, M., Kontkanen, J., Lehtipalo, K., and Kulmala, M.: Major contribution of neutral clusters to new particle formation in the free troposphere, Atmos. Chem. Phys. Discuss., 14, 18355–18388, doi:10.5194/acpd-14-18355-2014, 2014.

Rose, C., Sellegri, K., Velarde, F., Moreno, I., Ramonet, M., Weinhold, K., Krejci, R., Andrade, M., Wiedensohler, A., and Laj, P.: Frequent nucleation events at the high altitude station of Chacaltaya (5240 m a.s.l.), Bolivia, Atmos. Environ., 102, 18–29, doi:10.1016/j.atmosenv.2014.11.015, 2015.

Rosenfeld, D., Sherwood, S., Wood, R., and Donner, L.: Climate effects of aerosol–cloud interactions, Science, 343, 379–380, doi:10.1126/science.1247490, 2014.

Schobesberger, S., Väänänen, R., Leino, K., Virkkula, A., Backman, J., Pohja, T., Siivola, E., Franchin, A., Mikkilä, J., Paramonov, M., Aalto, P. P., Krejci, R., Petäjä, T., and Kulmala, M.: Airborne measurements over the boreal forest of southern Finland during new particle formation events in 2009 and 2010, Boreal Environ. Res., 18, 145–163, 2013.

Seidel, D. J., Ao, C. O., and Li, K.: Estimating climatological planetary boundary layer heights from radiosonde observations: comparison of methods and uncertainty analysis, J. Geophys. Res.-Atmos., 115, D16113, doi:10.1029/2009JD013680, 2010.

ACPD
15, 8151–8189, 2015

Sellegri, K., Yoon, Y. J., Jennings, S. G., O'Dowd, C. D., Pirjola, L., Cautenet, S., Chen, H., and Hoffmann, T.: Quantification of coastal new ultra-fine particles formation from in situ and chamber measurements during the BIOFLUX campaign, Environ. Chem., 2, 260–270, 2005.

Sihto, S.-L., Kulmala, M., Kerminen, V.-M., Dal Maso, M., Petäjä, T., Riipinen, I., Korhonen, H., Arnold, F., Janson, R., Boy, M., Laaksonen, A., and Lehtinen, K. E. J.: Atmospheric sulphuric acid and aerosol formation: implications from atmospheric measurements for nucleation and early growth mechanisms, Atmos. Chem. Phys., 6, 4079–4091, doi:10.5194/acp-6-4079-2006, 2006.

Suni, T., Kulmala, M., Hirsikko, A., Bergman, T., Laakso, L., Aalto, P. P., Leuning, R., Cleugh, H., Zegelin, S., Hughes, D., van Gorsel, E., Kitchen, M., Vana, M., Hõrrak, U., Mirme, S., Mirme, A., Sevanto, S., Twining, J., and Tadros, C.: Formation and characteristics of ions and charged aerosol particles in a native Australian Eucalypt forest, Atmos. Chem. Phys., 8, 129–139, doi:10.5194/acp-8-129-2008, 2008.

Tao, W.-K., Chen, J.-P., Li, Z., Wang, C., and Zhang, C.: Impact of aerosols on convective clouds and precipitation, Rev. Geophys., 50, RG2001, doi:10.1029/2011RG000369, 2012.

Tunved, P., Nilsson, E. D., Hansson, H.-C., Ström, J., Kulmala, M., Aalto, P., and Viisanen, Y.: Aerosol characteristics of air masses in northern Europe: Influences of location, transport, sinks, and sources, J. Geophys. Res., 110, D07201, doi:10.1029/2004JD005085, 2005.

Vaattovaara, P., Huttunen, P. E., Yoon, Y. J., Joutsensaari, J., Lehtinen, K. E. J., O'Dowd, C. D., and Laaksonen, A.: The composition of nucleation and Aitken modes particles during coastal nucleation events: evidence for marine secondary organic contribution, Atmos. Chem. Phys., 6, 4601–4616, doi:10.5194/acp-6-4601-2006, 2006.

Weber, R. J., Clarke, A. D., Litchy, M., Li, J., Kok, G., Schillawski, R. D., and McMurry, P. H.: Spurious aerosol measurements when sampling from aircraft in the vicinity of clouds, J. Geophys. Res., 103, 28337–28346, doi:10.1029/98JD02086, 1998.

Weigel, R., Hermann, M., Curtius, J., Voigt, C., Walter, S., Böttger, T., Lepukhov, B., Belyaev, G., and Borrmann, S.: Experimental characterization of the COndensation PArticle counting System for high altitude aircraft-borne application, Atmos. Meas. Tech., 2, 243–258, doi:10.5194/amt-2-243-2009, 2009.

Wiedensohler, A., Cheng, Y. F., Nowak, A., Wehner, B., Achtert, P., Berghof, M., Birmili, W., Wu, Z. J., Hu, M., and Zhu, T.: Rapid aerosol particle growth and increase of cloud condensation nucleus activity by secondary aerosol formation and condensation: A case

ACPD
15, 8151–8189, 2015

study for regional air pollution in northeastern China, J. Geophys. Res., 114, D00G08, doi:10.1029/2008JD010884, 2009.

Yli-Juuti, T., Nieminen, T., Hirsikko, A., Aalto, P. P., Asmi, E., Hõrrak, U., Manninen, H. E., Patokoski, J., Dal Maso, M., Petäjä, T., Rinne, J., Kulmala, M., and Riipinen, I.: Growth rates of nucleation mode particles in Hyytiälä during 2003–2009: variation with particle size, season, data analysis method and ambient conditions, Atmos. Chem. Phys., 11, 12865–12886, doi:10.5194/acp-11-12865-2011, 2011.

Young, L.-H., Benson, D. R., Montanaro, W. M., Lee, S.-H., Pan, L. L., Rogers, D. C., Jensen, J., Stith, J. L., Davis, C. A., Campos, T. L., Bowman, K. P., Cooper, W. A., and Lait, L. R.: Enhanced new particle formation observed in the northern midlatitude tropopause region, J. Geophys. Res., 112, D10218, doi:10.1029/2006JD008109, 2007.

ACPD
15, 8151–8189, 2015

Table 1. Overview of ATR-42 flights performed during the HYMEX campaign between the 11 September and the 4 November 2012 and discussed in the present study. The range of latitudes (respectively longitudes) corresponds to the minimum and maximum latitudes (respectively longitudes) reached during the flight. Dominant air mass origins are reported in the last column according to the following contractions: WE for Western Europe, SMS for Southern Mediterranean Sea, EMS for Eastern Mediterranean Sea and NE for Northern Europe.

Date	Take-off – Landing times (UTC)	Flight number	Range of latitudes	Range of longitudes	Dominant air mass origin
12 Sep 2012	10:10–12:51	34	43.5456–45.0286	2.8660–4.7834	WE
12 Sep 2012	08:19–09:21	35	42.5497–43.6403	3.9525–9.4847	WE
12 Sep 2012	10:42–14:20	36	42.5390–45.4146	7.8651–13.4646	WE
12 Sep 2012	15:22–16:49	37	42.5700–43.5800	3.9678–9.5748	WE
13 Sep 2012	19:55–20:40	38	43.4635–43.7027	3.9490–4.3397	NE
23 Sep 2012	14:12–17:18	39	42.4688–43.5495	3.5163–6.6463	WE
26 Sep 2012	06:09–09:32	40	42.2836–43.5358	4.0795–7.1505	WE
28 Sep 2012	14:57–20:26	41	39.0247–43.5556	1.1929–4.7809	SMS
02 Oct 2012	19:43–22:11	42	43.5345–43.7472	3.9718–4.3507	WE
11 Oct 2012	06:18–09:51	43	41.5560–43.6521	3.7292–6.0734	WE
12 Oct 2012	01:10–04:22	44	40.1657–43.6594	3.9816–11.6052	WE
12 Oct 2012	05:43–07:05	45	42.6541–43.4451	4.2909–9.5552	WE
14 Oct 2012	08:19–11:34	46	40.0262–43.6537	2.1463–7.9019	WE
14 Oct 2012	13:05–15:31	47	39.7553–43.5284	4.0702–5.3839	SMS
15 Oct 2012	05:16–06:33	48	42.5505–43.6523	3.9556–9.5761	SMS
15 Oct 2012	07:47–10:59	49	37.9256–42.8283	9.4726–13.0133	SMS/WE
15 Oct 2012	12:25–13:49	50	42.6096–43.5476	4.0322–9.5697	North/WE
18 Oct 2012	15:35–19:11	51	41.8076–43.5819	3.9640–6.6005	SMS
20 Oct 2012	09:54–12:56	52	38.1726–43.5235	1.3788–4.6854	SMS
20 Oct 2012	14:14–15:19	53	39.7616–43.6066	3.9778–4.6306	SMS
25 Oct 2012	19:12–22:18	54	38.7128–43.5761	1.2494–4.6609	SMS/WE
26 Oct 2012	23:25–01:24	55	39.8828–43.6801	0.2893–4.1770	WE
27 Oct 2012	05:52–09:18	56	41.2303–43.6439	3.9513–7.2013	WE
29 Oct 2012	14:06–16:33	57	43.4495–43.7011	3.9438–4.3705	NE
30 Oct 2012	21:41–01:16	58	41.2096–43.6470	3.9474–7.0443	Local
31 Oct 2012	02:24–05:29	59	40.8767–43.2733	4.9027–10.4004	SMS
03 Nov 2012	08:01–11:35	60	41.9706–43.6533	3.9881–8.0024	WE
04 Nov 2012	10:06–12:29	61	41.9660–43.6798	3.8330–8.1176	WE

ACPD
15, 8151–8189, 2015

Table 2. Nucleation probability and N_{5-10} concentration (statistics only include N_{5-10} above the threshold value) as a function of air mass origin.

Air mass origin	Nucleation probability (%)	N_{5-10} (cm^{-3})		
		Median	25th percentile	75th percentile
Northern Europe	60	342	269	1312
Western Europe	22	313	233	565
Southern Med. Sea	32	362	236	560
Eastern Med. Sea	0.3	531	286	636
Local	11	300	243	333

ACPD
15, 8151–8189, 2015

Table A1. Parameters of the Gaussians used to fit the SMPS size distributions as a function of daytime for the altitude ranges above 2000 m.

(a) 05:00–11:00 UTC			
Mode	Parameters	2000–3000 m	> 3000 m
M1	N (cm^{-3})	126.3 ± 70.4	200.3 ± 117.9
	σ	1.32 ± 0.01	1.34 ± 0.03
	d_p (nm)	30.5 ± 3.0	23.5 ± 3.7
M2	N (cm^{-3})	211.3 ± 130.1	78.1 ± 62.5
	σ	1.36 ± 0.02	1.37 ± 0.01
	d_p (nm)	51.6 ± 5.1	46.1 ± 7.6
M3	N (cm^{-3})	130.4 ± 88.0	49.1 ± 23.8
	σ	1.37 ± 0	1.37 ± 0
	d_p (nm)	99.7 ± 9.5	93.7 ± 8.7
M4	N (cm^{-3})	30.9 ± 26.9	9.6 ± 9.2
	σ	1.35 ± 0.05	1.31 ± 0.03
	d_p (nm)	205.4 ± 13.7	205.0 ± 9.7
(b) 11:00–17:00 UTC			
Mode	Parameters	2000–3000 m	> 3000 m
M1	N (cm^{-3})	248.1 ± 130.0	155.1 ± 126.0
	σ	1.32 ± 0.02	1.34 ± 0.03
	d_p (nm)	28.6 ± 3.6	24.6 ± 4.8
M2	N (cm^{-3})	161.8 ± 174.4	83.5 ± 46.9
	σ	1.36 ± 0.02	1.37 ± 0.01
	d_p (nm)	52.4 ± 5.8	49.7 ± 7.4
M3	N (cm^{-3})	150.8 ± 124.7	67.4 ± 36.0
	σ	1.38 ± 0.01	1.37 ± 0.01
	d_p (nm)	99.7 ± 8.9	97.5 ± 10.0
M4	N (cm^{-3})	39.0 ± 38.6	17.7 ± 19.4
	σ	1.35 ± 0.04	1.32 ± 0.04
	d_p (nm)	201.9 ± 12.7	224.3 ± 48.4
(c) 17:00–05:00 UTC			
Mode	Parameters	2000–3000 m	> 3000 m
M1	N (cm^{-3})	224.9 ± 156.7	176.6 ± 117.7
	σ	1.32 ± 0.02	1.33 ± 0.03
	d_p (nm)	27.7 ± 3.1	23.8 ± 3.5
M2	N (cm^{-3})	227.2 ± 169.4	136.9 ± 9.9
	σ	1.37 ± 0	1.37 ± 0
	d_p (nm)	50.6 ± 4.1	46.4 ± 5.6
M3	N (cm^{-3})	167.3 ± 108.7	61.4 ± 58.4
	σ	1.36 ± 0.01	1.35 ± 0.02
	d_p (nm)	101.6 ± 7.7	102.8 ± 8.4
M4	N (cm^{-3})	44.7 ± 40.7	9.2 ± 6.2
	σ	1.37 ± 0.05	1.39 ± 0.04
	d_p (nm)	216.4 ± 17.9	240.3 ± 12.1

ACPD
15, 8151–8189, 2015

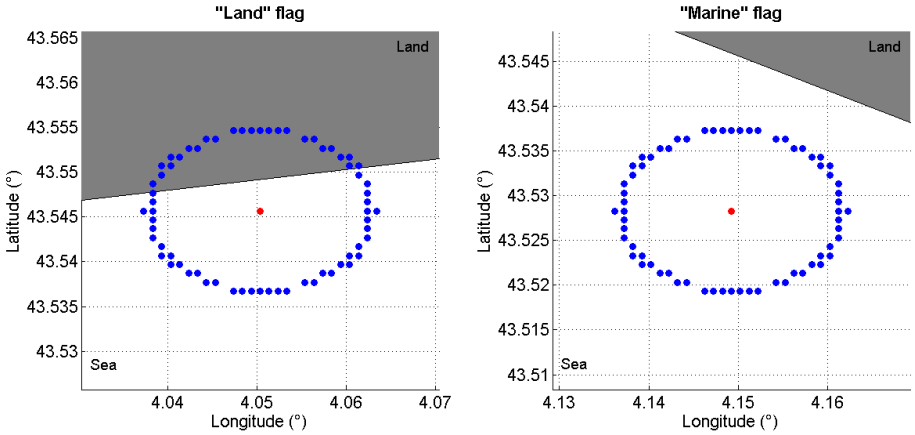

Figure 1. Method for the determination of the “marine”/”land” flag. The red point corresponds to the location of the aircraft. The blue points represent the 1000 ± 50 m minimum distance from land required for a measurement to be considered as “marine”.

ACPD
15, 8151–8189, 2015

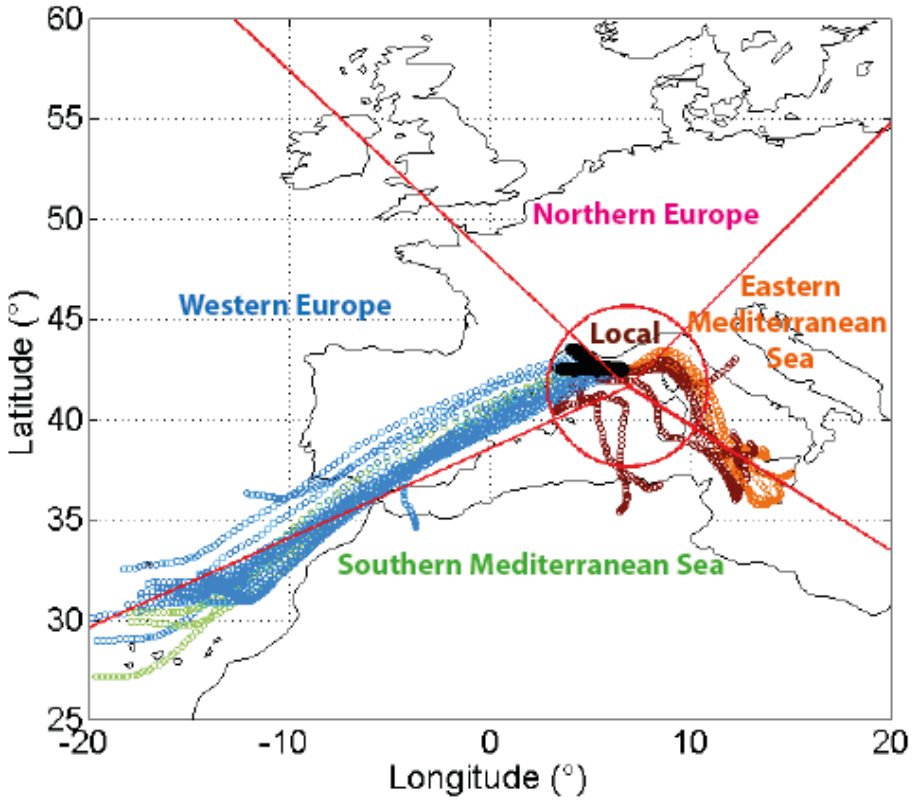

Figure 2. Illustration of the air mass back trajectories calculation along the flight path (black points) for flight 39 (23 September 2012). Sectors used for the air mass origin analysis are also shown.

ACPD
15, 8151–8189, 2015

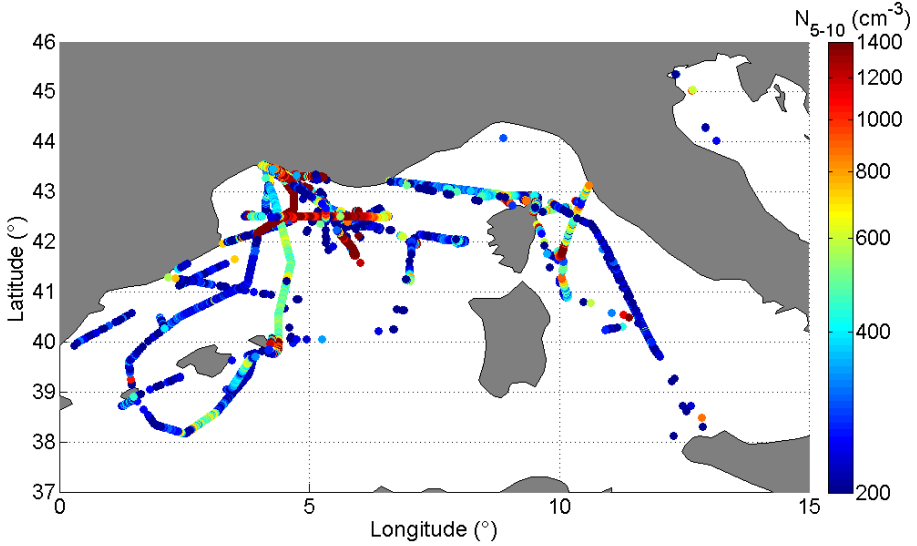

Figure 3. Location of $N_{5–10}$ concentrations exceeding the threshold value of 175 cm^{-3}. Lower and upper limit of the colour scale were set to the 10th and 90th percentile of $N_{5–10}$ concentration, respectively.

ACPD
15, 8151–8189, 2015

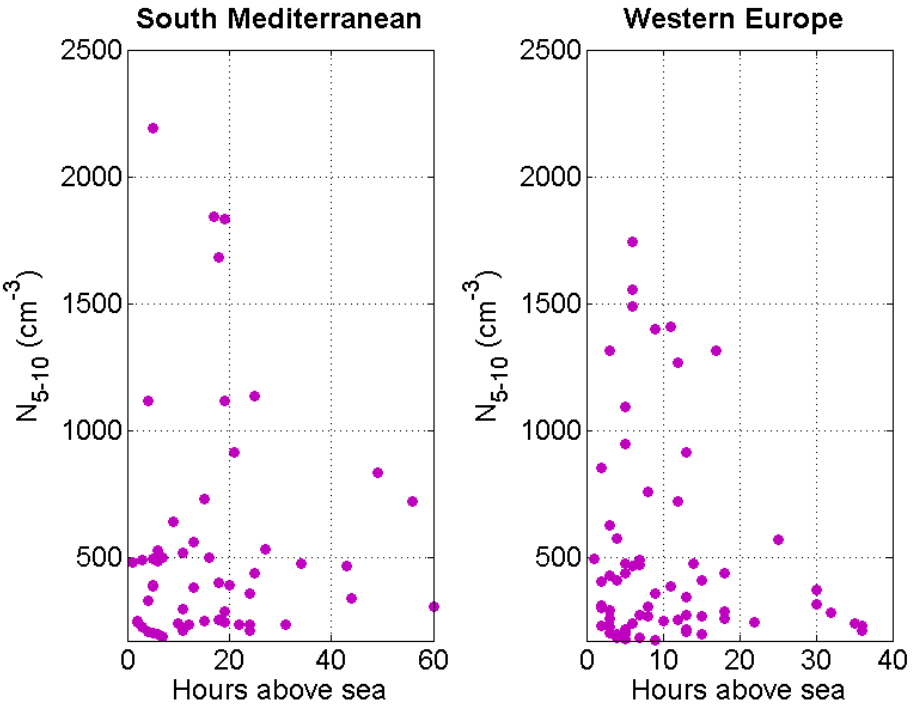

Figure 4. N_{5-10} concentrations as a function of air mass fetch, separately for Southern Mediterranean Sea and Western Europe air masses.

ACPD
15, 8151–8189, 2015

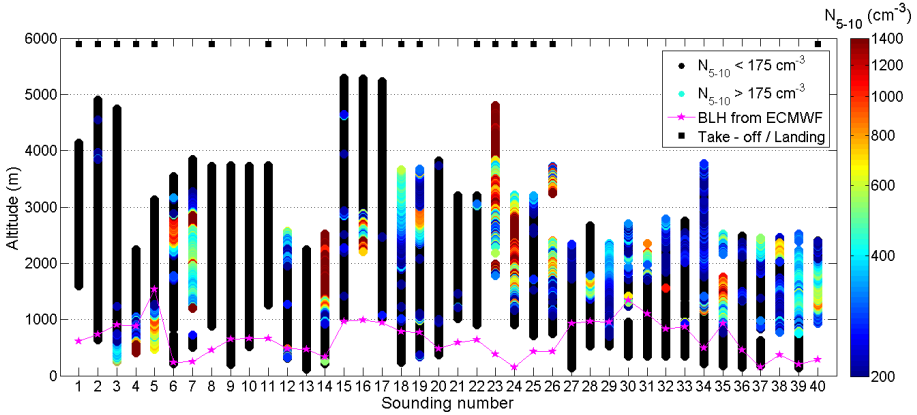

Figure 5. Profile of the $N_{5–10}$ concentrations during the ATR-42 soundings performed in clear sky conditions above the sea. Lower and upper limit of the colour scale were set to the 10th and 90th percentile of $N_{5–10}$ concentration, respectively. Pink stars and line corresponds to the ECMWF boundary layer height. Black rectangles highlight soundings performed during take-off or landing phase.

ACPD
15, 8151–8189, 2015

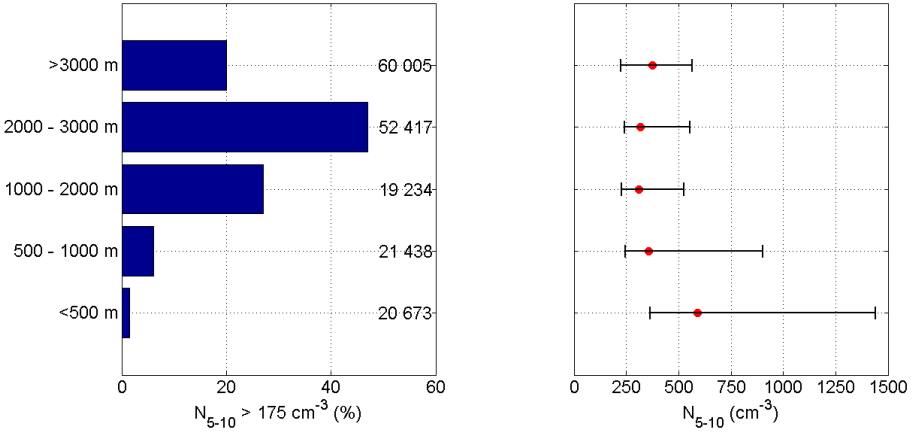

Figure 6. Statistics on the detection of significant particle concentration in the size range 5–10 nm as a function of altitude (left panel, the number of data points is indicated on the plot for each altitude range). Corresponding median concentrations are reported on the right panel; left and right limits of the error bars stand for the 1st and 3rd quartile, respectively.

ACPD
15, 8151–8189, 2015

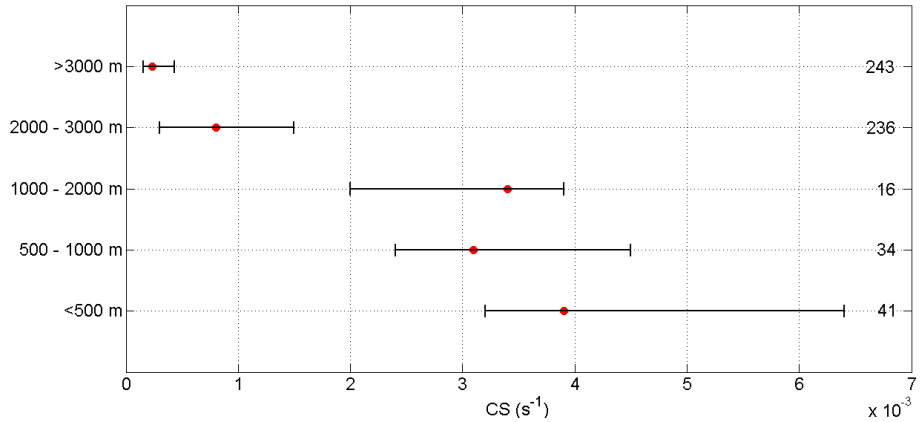

Figure 7. Median CS as a function of altitude range; left and right limits of the error bars stand for the 1st and 3rd quartile, respectively. The number of data points included in the statistics is indicated on the plot for each altitude range.

ACPD
15, 8151–8189, 2015

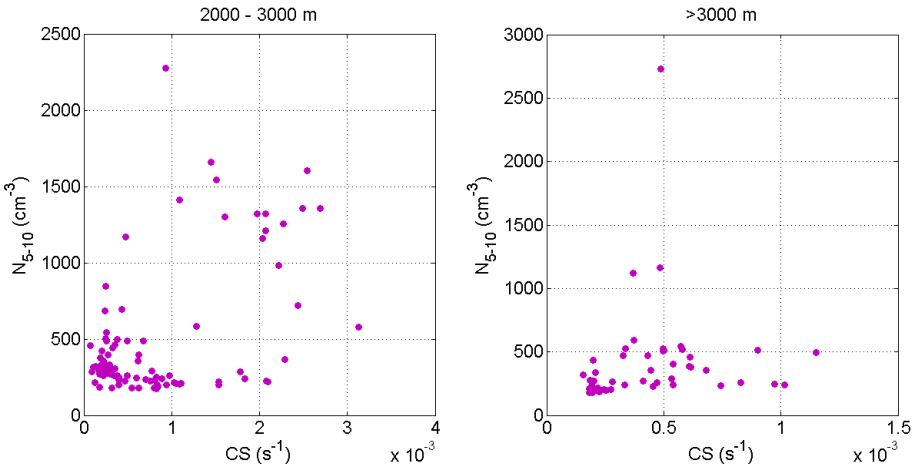

Figure 8. Particle concentration in the size range 5–10 nm as a function of condensation sink (CS) for altitude ranges above 2000 m.

ACPD
15, 8151–8189, 2015

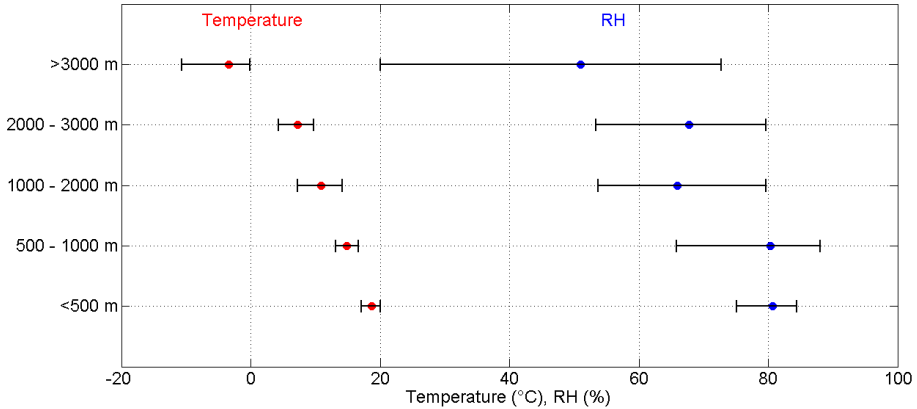

Figure 9. Median temperature and relative humidity (RH) as a function of altitude range; left and right limits of the error bars stand for the 1st and 3rd quartile, respectively.

ACPD
15, 8151–8189, 2015

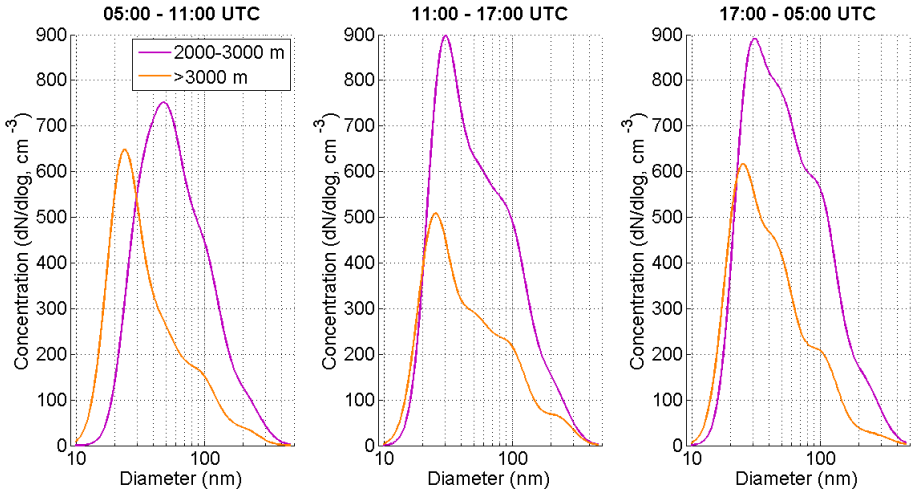

Figure 10. Averaged fitted SMPS size distributions as a function of daytime and altitude.

ACPD
15, 8151–8189, 2015

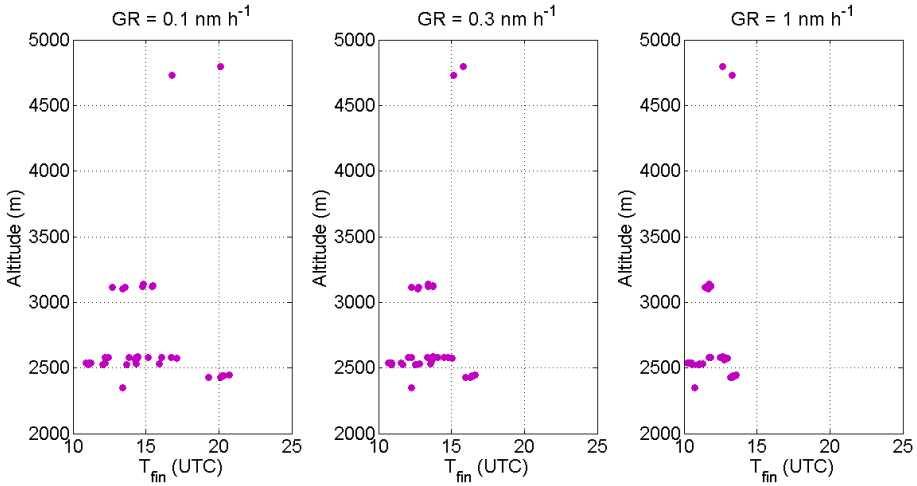

Figure 11. Estimations of t_{fin}, the time at which $N_{5–10}$ concentrations reach half of their initial values, as a function of altitude and particle growth rate.

ACPD
15, 8151–8189, 2015